Templating Hollow Polymeric Spheres from Catanionic Equilibrium Vesicles: Synthesis and Characterization

C. A. McKelvey,† E. W. Kaler,† J. A. Zasadzinski,‡ B. Coldren,‡ and H.-T. Jung‡

Department of Chemical Engineering, Center for Molecular Engineering and Thermodynamics, University of Delaware, Newark, Delaware 19716, and Department of Chemical Engineering, University of California at Santa Barbara, Santa Barbara, California

Received April 14, 2000. In Final Form: July 18, 2000

Hollow polymer spheres of styrene and divinyl benzene can be templated from catanionic equilibrium vesicles formed by cetyltrimethylammonium tosylate (CTAT) and sodium dodecylbenzenesulfonate (SDBS) or cetyltrimethylammonium bromide (CTAB) and sodium octyl sulfate (SOS). Characterization by many methods suggests the microstructure of the equilibrium vesicle template is left largely intact in the final polymer product. The particles have an average radius of ca. 60 nm and a membrane shell less than 10 nm thick. The cross-linked hollow polymer vesicles are robust and withstand complete drying and resuspension in water with no apparent change in microstructure. The polymer membrane surfaces can be functionalized by sulfonation or surfactant adsorption, and this functionalization prevents aggregation of the polymer particles when they are resuspended in water.

Introduction

Vesicles are candidates for a variety of controlled release applications because they compartmentalize the aqueous domain on submicron length scales. Vesicles can be used as drug delivery[1,2] and gene therapy vehicles,[3,4] even for humans,[5] as well as for a surprisingly wide range of other applications.[6] Useful vesicle formulations need to be stable, inexpensive, and versatile, especially with regard to control of dimensions and surface characteristics. Surface functionalization has a profound influence on stability, both in regard to mechanical degradation and to colloidal aggregation resistance.

Vesicles investigated for applications are almost exclusively kinetically stabilized. These transient microstructures can be formed by sonication,[7−10] extrusion,[11] detergent dialysis,[7,12] reverse-phase evaporation,[7] and pH changes.[13] The properties of kinetically stabilized vesicles generally depend on how they are produced (e.g., the length of sonication or the rate of extrusion), and they will inherently revert back to their native lamellar phase state over time. The surfactants used are relatively expensive and are often of biologic origin.

A simpler and more economical method to produce vesicles is by mixing cationic and anionic surfactants. The resulting "catanionic" vesicles form spontaneously, and the bilayers are the equilibrium state of aggregation.[14] The particular surfactants used and their relative concentrations govern the size and bilayer thickness of catanionic vesicles. Both the phase behavior and microstructure of several catanionic systems have been investigated.[15−19] Catanionic vesicles have not found wide use in applications. The equilibrium structures are stable indefinitely, but changes in solution environment (e.g., salt concentration and pH) cause drastic transformations of microstructure. Similarly stable vesicles have been reported by Szleifer et al.[20]

Thus the major shortcoming of both kinetically stabilized and equilibrium vesicles is their inherent mechanical instability in response to environmental changes. To overcome this, many groups have attempted to polymerize vesicles to produce a more robust polymer membrane that would resist degradation. Most vesicle polymerization studies to date involve the polymerization of "hand-made" surfactants that contain a polymerizable group.[21−29] The

† University of Delaware.
‡ University of California.

(1) McIntosh, D. P.; Heath, T. D. *Biochim. Biophys. Acta* **1982**, *690*, 224−230.
(2) Hashimoto, Y.; Sugawara, M.; Masuko, T.; Hojo, H. *Cancer Res.* **1983**, *43*, 5328−5334.
(3) Fraley, R.; Subramani, S.; Berg, P.; Papahadjopoulos, D. *J. Biol. Chem.* **1980**, *255*, 10431−10435.
(4) Wilson, T.; Papahadjopoulos, D.; Taber, R. *Cell* **1979**, *17*, 77−84.
(5) Allen, T. M. *Curr. Opin. Colloid Interface Sci.* **1996**, *1*, 645−651.
(6) Lasic, D. D. *Liposomes: from Physics to Applications*; Elsevier Science Publishers: New York, 1993.
(7) Szoka, F.; Papahadjopoulos, D. *Annu. Rev. Biophys. Bioeng.* **1980**, *9*, 467−508.
(8) Papahadjopoulos, D.; Miller, N. *Biochim. Biophys. Acta* **1967**, *135*, 624−638.
(9) Huang, C. H. *Biochemistry* **1969**, *8*, 344−351.
(10) Nozaki, Y.; Lasic, D. D.; Tanford, C.; Reynolds, J. A. *Science* **1982**, *217*, 366−367.
(11) Mayer, L. D.; Hope, M. J.; Cullis, P. R. *Biochim. Biophys. Acta* **1986**, *858*, 161−168.
(12) Kagawa, Y.; Racker, E. *J. Biol. Chem.* **1971**, *246*, 5477−5487.
(13) Hauser, H.; Mantsch, H. H.; Casal, H. L. *Biochemistry* **1990**, *29*, 2321−2329.
(14) Kaler, E. W.; Murthy, A. K.; Rodriguez, B. E.; Zasadzinski, J. A. N. *Science* **1989**, *245*, 1371−1374.
(15) Marques, E.; Khan, A.; Miguel, M. D.; Lindman, B. *J. Phys. Chem.* **1993**, *97*, 4729−4736.
(16) Talhout, R.; Engberts, B. F. N. *Langmuir* **1997**, *13*, 5001−5006.
(17) Kaler, E. W.; Herrington, K. L.; Murthy, A. K.; Zasadzinski, J. A. N. *J Phys. Chem.* **1992**, *96*, 6698−6709.
(18) Yatcilla, M. T.; Herrington, K. L.; Brasher, L. L.; Kaler, E. W.; Chiruvolu, S.; Zasadzinski, J. A. N. *J. Phys. Chem.* **1996**, *100*, 5874−5879.
(19) Brasher, L. L.; Kaler, E. W. *Langmuir* **1996**, *12*, 6270−6276.
(20) Szleifer, I.; Gerasimov, O. V.; Thompson, D. H. *Proc. Natl. Acad. Sci. U.S.A.* **1998**, *95*, 1032−1037.
(21) Sisson, T. M.; Lamparski, H. G.; Kölchens, S.; Elayadi, A.; O'Brien, D. F. *Macromolecules*, **1996**, *29*, 8321−8329.
(22) Dvolaitzky, M.; Guedeau-Boudeville, M. A.; Léger, L. *Langmuir* **1992**, *8*, 2595−2597.
(23) Abid, S. K.; Sherrington, D. C. *Polymer* **1992**, *33*, 175−180.
(24) Guo, C. Y.; Shankar, R. R.; Cai, S. H.; Wu, J. Q.; Abe, S.; Thomas, R. N.; Kuo, J. E. *Langmuir* **1992**, *8*, 815−823.
(25) Kunitake, T.; Nakashima, N.; Kunitake, M. *Macromolecules* **1989**, *22*, 3544−3550.
(26) Peek, B. M.; Callahan, J. H.; Namboodiri, K.; Singh, A.; Gaber, B. P. *Macromolecules* **1994**, *27*, 292−297.
(27) Cho, I.; Dong, S.; Jeong, S. W. *Polymer* **1995**, *36*, 1513−1515.

10.1021/la000569d CCC: $19.00
Published on Web 09/28/2000

surfactants used in these studies are generally expensive and not widely available.

An alternative to surfactant polymerization is to use the vesicle architecture as a template for polymerization. In this case, common hydrophobic monomers are added to swell the bilayers of a vesicle solution and are subsequently polymerized. The goal is to capture or template the vesicle structure in order to form hollow polymer spheres. There have been several attempts to polymerize a monomer incorporated into the bilayer of kinetically stabilized vesicles. In these studies, four groups have claimed some success in capturing the features of the original vesicle templates[30−33] although one of these groups has since presented more detailed results which suggest the formation of solid latex polymer particles rather than the desired hollow polymer vesicles.[34] Thus our goal is to develop an inexpensive and practical technique for producing hollow polymer spheres that combines the efficiency and ease of making equilibrium vesicles with the structural integrity that polymerization provides.

Two common monomers are used, styrene and divinylbenzene, and they swell the bilayers of equilibrium vesicles made of either cetyltrimethylammonium tosylate (CTAT) and sodium dodecylbenzenesulfonate (SDBS) or cetyltrimethylammonium bromide (CTAB) and sodium octyl sulfate (SOS).[35] Using a combination of styrene and divinylbenzene allows adjustment of the cross-linking density without altering the chemical composition of the final polymer. Once polymerized, the free surfactants are removed from the mixture by dialysis. The polymerized particles immediately aggregate upon removal of the surfactant, so two surface modifications were developed to produce stable aqueous solutions upon resuspension of the polymer particles.

The first modification is sulfonation of the aromatic rings in the polymer, which produces an electrostatic repulsion between the particles. The second approach is to produce sterically stabilized vesicles by adsorbing nonionic surfactant to the surface of the particles. In both cases, the stabilized particles could be completely dried and resuspended to form stable dispersions.

Experimental Section

Materials. Both CTAT and CTAB were purchased from either Sigma or Aldrich Chemical Co. and recrystallized three times from a 1:1 mixture of ethanol and acetone. SDBS was purchased from TCI America. SOS from Acros was treated with a SEP-PAK C18 Cartridge from Waters Assoc. to remove surface-active impurities.[36] The cartridge was pretreated with 2 mL of ethanol and then 5 mL of water before flowing a 10 wt % aqueous SOS solution through it.[37] The first 1 mL of the elluent was discarded and each cartridge treated 20 mL total. Divinylbenzene and styrene were purchased from Scientific Polymer Products. Both were vacuum distilled to remove oligomers and inhibitors prior use. The monomers were kept in amber vials at 3 °C. Water was distilled and deionized. The initiator, 2,2'-Azobis (2-amidinopropane) dihydrochloride (V-50), was purchased from Wako Chemicals; any storage was at 3−5 °C. Spectra/Por regenerated dialysis tubing with a molecular weight cutoff of 15000 Da was purchased from Fisher Scientific and rinsed in deionized water before use. Sulfuric acid (99.999%), phosphorus pentoxide (99.99+%), Brij 700 ($\sim C_{18}E_{100}$), Brij 35 ($\sim C_{12}E_{23}$), Brij 58 ($\sim C_{16}E_{20}$), and Brij 78 ($\sim C_{18}E_{20}$) were purchased from Aldrich. Octaethylene glycol mono-*n*-dodecyl ether ($C_{12}E_8$), pentaethylene glycol mono-*n*-dodecyl ether ($C_{12}E_5$), and hexaethylene glycol mono-*n*-dodecyl ether ($C_{12}E_6$) were purchased from Nikko Chemicals Co. (Tokyo, Japan). Potassium hydroxide pellets were purchased from Sigma. HPLC grade methanol, ethanol, and acetone were purchased from Fisher Chemicals. All materials were used as received except where noted.

Quasi-Elastic Light Scattering (QELS). QELS was performed at 25 °C with a Brookhaven model BI-200SM goniometer, Brookhaven model BI-9000AT correlator, and a Lexel 300 mW Ar laser. All experiments were performed at 90°, and the autocorrelation function was analyzed by the method of cumulants.[38] The apparent hydrodynamic radius was obtained from the measured diffusion coefficient using the Stokes−Einstein relationship.

Small-Angle Neutron Scattering (SANS). SANS measurements were made at the National Institute of Standards and Technology (NIST) in Gaithersburg, MD. An average radiation wavelength of 6 Å with a spread of 11% was used. Samples were held at 25 °C in quartz "banjo" cells with 1 mm path lengths. Three sample−detector distances were used to give a range in scattering vector of 0.005−0.5 $Å^{-1}$. The data were corrected for detector efficiency, background, and empty cell scattering and placed on an absolute scale using NIST procedures.

Cryogenic Transmission Electron Microscopy (Cryo TEM). A 5 μL drop of sample was applied to a holey carbon film supported on a copper grid (Lacey-substrate, made by Ted Pella of Redding, CA) in a controlled environment vitrification system (CEVS) at 25 °C. This CEVS setup is described in detail by Bellare et al.[39] The grid was held by a pair of tweezers attached to a spring-loaded arm. Using a swab of filter paper the grid was carefully blotted to achieve the appropriate surface thickness (50−500 nm). The sample was then rapidly plunged into a container of liquid ethane and propane (50:50 mix) cooled by a liquid-nitrogen bath. The grid was transferred under liquid nitrogen to a Gatan model 626 cold-stage and held between −168 and −170 °C during imaging. Imaging was performed at 100 kV with a model 2000 FX JEOL TEM under low electron doses to prevent sample deterioration. Images were captured on SO-163 plates at underfocus conditions and developed for 12 min using full-strength D-19 developer (Kodak).

Sonication. Samples were directly sonicated in 20 mL scintillation vials for 15 min in an ice bath using a Heat Systems Ultrasonics model W-225 sonicator. The mixtures were then centrifuged for 3 h at 25 °C, and the supernatant was removed for further characterization.

Equilibrium Vesicle Formation. Vesicle phases were contained in either 250 mL round-bottom flasks or 40 mL scintillation vials with PTFE lined septum tops. The catanionic mixtures were prepared by adding water directly to measured amounts of surfactant powders or mixing two stock solutions of the cationic and anionic surfactants, respectively. The compositions of interest here were 0.7 wt % CTAT and 0.3 wt % SDBS or 0.8 wt % CTAB and 1.2 wt % SOS. The mixtures were initially mixed by stirring with a Teflon-coated stir bar for 1 day. At least 2 weeks at ambient conditions was allowed for equilibration to occur, during which time the average hydrodynamic radius was monitored with QELS.

Polymerization. The vesicles were deoxygenated for 2 h by flowing humidified nitrogen (99.999%) through the headspace of

(28) Komatsu, T.; Tsuchida, E.; Böttcher, C.; Donner, D.; Messerschmidt, C.; Siggel, U.; Stocker, W.; Rabe, J. P.; Fuhrhop, J.-H. *J. Am. Chem. Soc.* **1997**, *119*, 11660−11665.
(29) Jung, M.; Ouden, den Ouden, I.; Montoya-Goñi, A.; Hubert, D. H. W.; Frederik, P. M., van Herck, A. M., German, A. L. *Langmuir* 2000, *16*, 4185−4195.
(30) Kurja, J.; Nolte, R. J. M.; Maxwell, I. A.; German, A. L. *Polymer* **1993**, *34*, 2045−2049.
(31) Hotz, J.; Meier, W. *Langmuir* **1998**, *14*, 1031−1036.
(32) Poulain, N.; Nakache, E.; Pina, A.; Levesque, G. *J. Polym. Sci., Part A: Polym. Chem.* **1996**, *34*, 729−737.
(33) Murthagh, J.; Thomas, J. K. *Faraday Discuss. Chem. Soc.* **1986**, *81*, 127−136.
(34) Jung, M.; Hubert, D. H. W.; Bomans, P. H. H.; Frederik, P. M.; Meuldijk, J.; van Herk, A. M.; Fischer, H.; German, A. L. *Langmuir* **1997**, *13*, 6877−6880.
(35) Morgan, J. D.; Johnson, C. A.; Kaler, E. W. *Langmuir* **1997**, *13*, 6447−6451.
(36) Rosen, M. J. In *Phenomena in Mixed Surfactant Systems*; Scamehorn, J. F., Ed.; American Chemical Society: Washington, DC, 1986.
(37) Herrington, K. L. Ph.D. Thesis, University of Delaware, 1994.
(38) Koppel, D. E. *J. Chem. Phys.* **1972**, *57*, 4814−4820.
(39) Bellare, J. R.; Davis, H. T.; Scriven, L. E.; Talmon, Y. *J. Electron Microsc. Tech.* **1988**, *10*, 87−111.

the container. The freshly distilled monomer was then injected with a syringe through a septum, and the mixture was vigorously stirred for 1 day. An additional 1 day was allowed for the swollen vesicles to age, and then they were heated to 65 °C in a water bath with slow stirring. Once the swollen vesicle solution reached 65 °C, 100 μL of freshly prepared 18 wt % aqueous V-50 was added via syringe through the septum to initiate polymerization. The solution was held at 65 °C for 8 h and then cooled to room temperature.

Sulfonation. Modification of the polymer surface began with the removal of free surfactant by methanol dialysis. The dialysis involved 100 g of polymerized vesicle solution inside of several dialysis tubes placed in approximately 1 L of methanol, which was changed every 12 h for 3 or 4 days. Methanol was used because dialysis against water is very slow. The particle mixtures in methanol were then vacuum-dried at 35 °C. A 5−6 g amount of sulfuric acid and 1 g of phosphorus pentoxide were added to each sample of 100−200 mg of dry polymer to add sulfonate groups to the aromatic rings of the polymer.[40] This mixture reacted 4 days before neutralization with potassium hydroxide. To remove salt created during neutralization, the mixtures were dialyzed in deionized water for at least 1 week following the methanol procedure above. Finally, the sulfonated polymer aggregates were resuspended in water by sonication yielding a clear blue solution over a white precipitate.

Steric Stabilization. Unsulfonated dialyzed particles were redispersed in water by adding a 0.1−2.0 wt % aqueous surfactant solution to the dry particles and waiting 2−3 days until a transparent blue solution formed. If an insufficient amount of surfactant was added, some particles remained on the bottom of the vial. Resuspension with the Brij surfactant solutions required sonication with the particles. Sonication of the Brij solutions in the absence of particles did not produce vesicles.

Results

Styrene and divinylbenzene can be added in amounts up to 12% of the total surfactant weight before any qualitative signs of microstructure changes are observed (e.g., formation of a meniscus with an oil phase or development of turbidity). This monomer loading is equivalent to 1 mol of monomer for every 3 mol of surfactant. CTAT/SDBS vesicles and CTAB/SOS vesicles have hydrodynamic radii of 60 and 50 nm, respectively, for the compositions of interest here. Monomer additions of up to 10% of the total surfactant weight can be made to these vesicles with no change in their hydrodynamic radius (QELS results not shown).

SANS measurements of CTAT/SDBS vesicles in D_2O with varying amounts of styrene and divinylbenzene yield similar results for each monomer (Figure 1). There is a slight increase in the scattered intensity as the amount of monomer is increased. At low values of q, a q^{-2} dependence is observed, which is a signature of bilayer structures. The calculated bilayer thickness from either a modified Guinier plot ($\ln[Iq^2]$ versus q^2) or the indirect Fourier transform method of Glatter[41] is 3.1 nm prior to monomer addition. Only a small increase (<10%) in the bilayer thickness is observed with the addition of either monomer. Cryo TEM pictures of CTAT/SDBS equilibrium vesicles with and without divinylbenzene are very similar (Figures 2 and 3). The hollow nature of the vesicles is clearly visible from these micrographs, and the vesicles generally appear to be spherical in shape.

No obvious qualitative changes in appearance occur during or immediately after polymerization, but small birefrigent "clouds" are often observed suspended in the

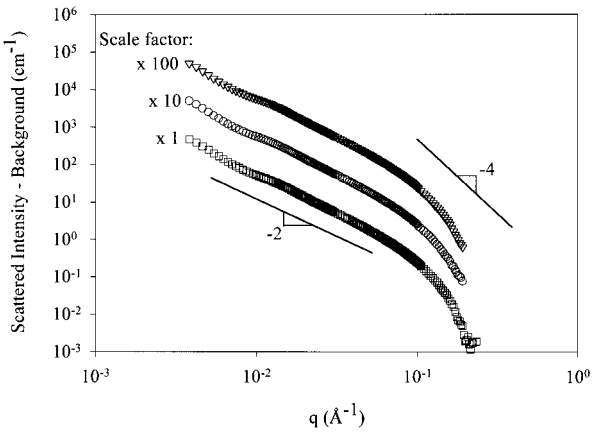

Figure 1. SANS data, $I - B$ (intensity minus background) versus q, for equilibrium vesicle samples with 0.7 wt % CTAT and 0.3 wt % SDBS with no divinylbenzene (□), 5.0% divinylbenzene with respect to surfactant weight (○), and 7.5% divinylbenzene with respect to surfactant weight (▽). The data sets are scaled for clarity with scale factors indicated in the inset. The low-q region decays as q^{-2} indicative of bilayer scattering for all of the spectra.

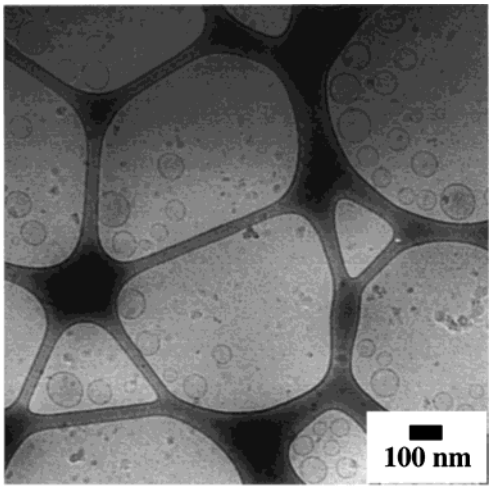

Figure 2. Cryo TEM electron micrograph of equilibrium vesicles with 0.7 wt % CTAT and 0.3 wt % SDBS and no added monomer. The vesicles here are polydisperse with an average hydrodynamic radius of 60 nm.

polymerized mixtures after long periods of time. QELS measurements of these samples are inconsistent, and occasionally the hydrodynamic diameters approach 200 nm (twice the equilibrium vesicle diameter) suggesting the presence of different morphologies. These morphological changes are due to alterations of the vesicle−vesicle interactions in solution as a result of either loss of electrostatic stability or entropic stability due to the stiffening of the bilayers by polymerization.[42] The inhomogeneities preclude the use of SANS or QELS to characterize the microstructure quantitatively. However, catanionic vesicles are micellized by the presence of their counterion salt[43] (e.g., sodium tosylate for the CTAT/SDBS vesicles) or the detergent Triton X-100. Addition of the surfactant counterion salt to polymerized catanionic vesicles results in a white precipitate in a clear solution. Addition of Triton X-100 to the polymerized mixtures produces a solution with a faint blue color.

(40) Vink, H. *Makromol. Chem*. **1981**, *182*, 279−281.
(41) *Small-Angle X-ray Scattering*; Glatter, O., Kratky, O., Eds.; Academic Press: London, 1982; pp 119−166.
(42) Jung, H.-T.; Coldren, B.; Zasadzinski, J. A.; Iampietro, D. J.; Kaler, E. W. Submitted for publication in *Science*.
(43) Brasher, L. L.; Herrington, K. L.; Kaler, E. W. *Langmuir* **1995**, *11*, 4267−4277.

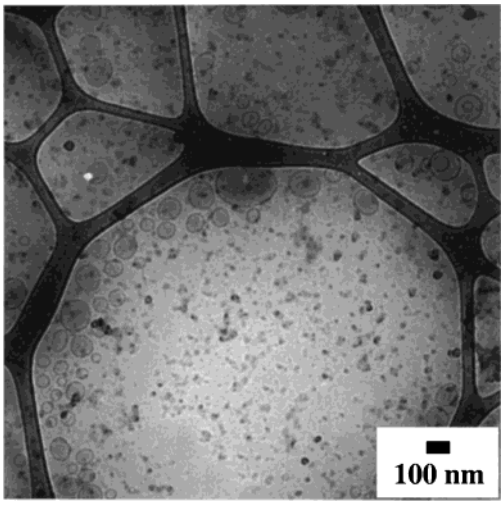

Figure 3. Cryo TEM electron micrograph of equilibrium vesicles with 0.7 wt % CTAT and 0.3 wt % SDBS with 7.5% divinylbenzene with respect to surfactant weight. The vesicle microstructure appears identical to the equilibrium vesicles without monomer in Figure 2.

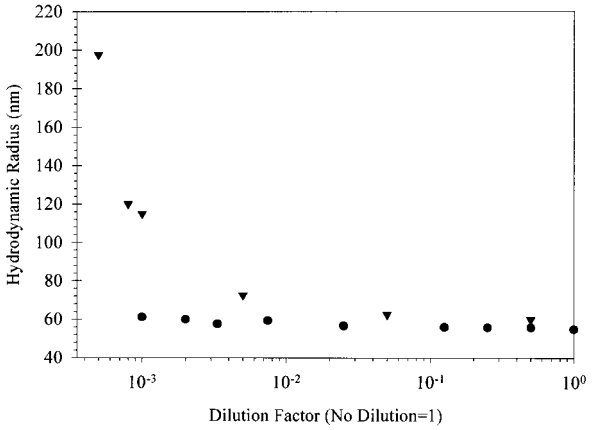

Figure 4. QELS data, hydrodynamic radius versus dilution factor. The hydrodynamic radius of equilibrium vesicles composed of 0.7 wt % CTAT and 0.3 wt % SDBS increases with dilution (▼). In contrast, the hydrodynamic radius of sulfonated polymerized particles remains constant (●).

The polymer particles immediately aggregate upon dialysis in methanol because the surfactant is removed. These surfactant-free particles are dried and sulfonated before redispersion in water. The solutions formed by this method are stable and appear blue to the eye. These aggregates have the same hydrodynamic radius as the unpolymerized vesicles. Because of their cross-linked polymer structure, the sulfonated polymerized vesicles have the same hydrodynamic radius regardless of dilution (Figure 4), while the radius of the parent CTAT/SDBS equilibrium vesicles increases with dilution since the vesicle composition depends on the overall composition.[17,19]

Systematic QELS and Cryo TEM experiments were performed with $C_{12}E_8$-stabilized particles. QELS of the $C_{12}E_8$-stabilized particles reveals a hydrodynamic radius identical to that of the original equilibrium vesicle radius, and the size does not change with dilution (results not shown). Cryo TEM images of these resuspended polymer particles show them to be hollow (Figure 5).

$C_{12}E_8$-stabilized polymer vesicles were also chosen for SANS experiments. The $C_{12}E_8$ SANS spectra are fitted with a polydisperse hard sphere form factor model[44,45]

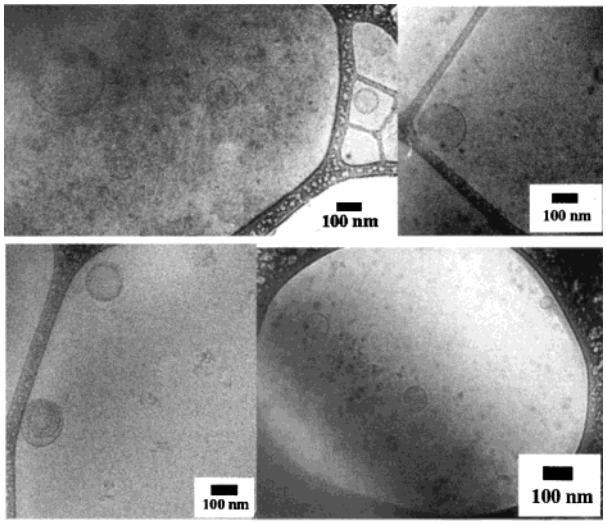

Figure 5. Cryo TEM electron micrographs of resuspended hollow polymer spheres coated with $C_{12}E_8$. A dilute sample was used here: 0.005 wt % polymer particles and 0.005 wt % $C_{12}E_8$. The particles are polydisperse and have an average hydrodynamic radius of 60 nm (from QELS)

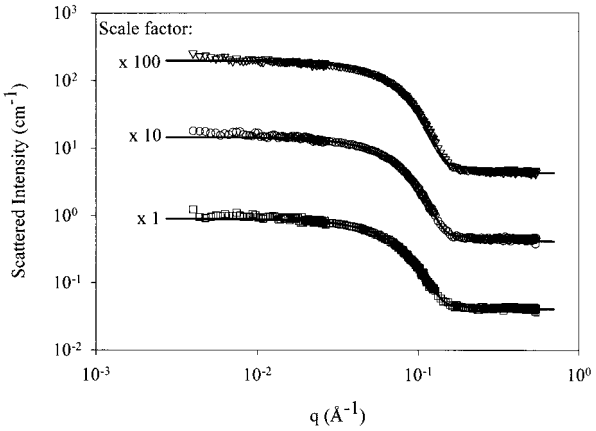

Figure 6. SANS data, I versus q, for $C_{12}E_8$ micelles in D_2O: 0.30 wt % $C_{12}E_8$ (□); 0.50 wt % $C_{12}E_8$ (○); 0.70 wt % $C_{12}E_8$ (▽). A polydisperse hard sphere model was fitted to each data set using three adjustable parameters—the radius, polydispersity, and surfactant micellar density, which are 2.57 nm, 0.165, and 0.92 g/cm^3, respectively. The data sets are scaled for clarity.

containing three adjustable parameters—radius, polydispersity, and volume fraction (Figure 6). The radius and polydispersity used for all three concentrations are 2.57 nm and 0.165, respectively. The fitted value of the volume fraction is 1.2 times the measured weight fraction, which implies a micellar density of 0.92 g/cm^3.

With polymer vesicles added, the SANS spectra are more complicated (Figure 7). The high-q region displays the characteristic pattern of $C_{12}E_8$ micelle scattering, but the low-q region shows a new pattern of scattering caused by the surfactant-coated polymer vesicles, including a q^{-2} dependence as is observed for the equilibrium vesicles.

A polydisperse core−shell model is used to fit the data in the low-q region, where the core is assumed to be D_2O and the (uniform) shell corresponds to the $C_{12}E_8$-coated polymer membrane. This model has four parameters—core radius, shell thickness, overall polydispersity, and a concentration scaling. The core radius, shell thickness, and overall polydispersity used for all four spectra (Figures

(44) Vrij, A. *J. Chem. Phys.* **1979**, *71*, 3267−3270.

(45) Griffith, W. L.; Triolo, R.; Compere, A. L. *Phys. Rev. A* **1987**, *35*, 2200−2206.

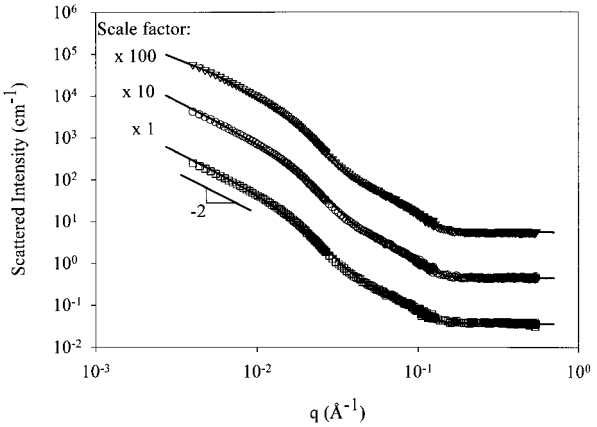

Figure 7. SANS data, *I* versus *q*, for polymerized particles with $C_{12}E_8$ in D_2O: 0.15 wt % polymer particles and 0.15 wt % $C_{12}E_8$ (□); 0.25 wt % polymer particles and 0.25 wt % $C_{12}E_8$ (○); 0.35 wt % polymer particles and 0.35 wt % $C_{12}E_8$ (▽). The model fits are a sum of the scattering from a polydisperse core shell model and the polydisperse hard sphere model used in the spectra of Figure 6. The data sets are scaled for clarity.

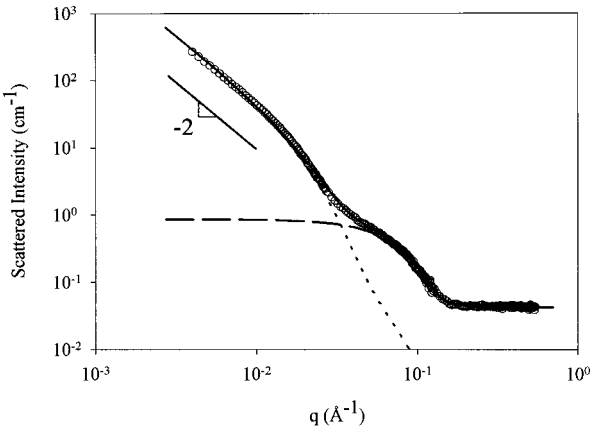

Figure 8. SANS data, *I* versus *q*, for polymerized particles with $C_{12}E_8$ in D_2O: 0.15 wt % polymer particles and 0.35 wt % $C_{12}E_8$ (○). The polydisperse hard sphere model (broad dashes) is identical to the model used in Figure 6. A polydisperse core−shell model has been added to take into account scattering from the polymer particles. The core−shell model had four parameters—core radius, shell thickness, overall polydispersity, and a shell density, which are 55.0 nm, 9.0 nm, 0.39, and 1.09 g/cm^3, respectively. The two models are added to obtain a fit to the data (solid line).

7 and 8) are 55.0 nm, 9.0 nm, and 0.39, respectively. A fitted membrane shell density of 1.09 g/cm^3, together with the modeled particle dimensions, relates the measured weight fractions to the model volume fractions.

Figure 8 demonstrates how the hard sphere and core shell models are added and illustrates how the scattering in the two extreme *q*-regimes can be attributed to scattering from micelles or the larger surfactant-coated polymer shells, respectively. The models for these two regions yield information about the aggregate size, geometry, and concentration for both populations.

Discussion

Both SANS and Cryo TEM suggest the equilibrium vesicle microstructure is unaffected by the presence of nearly 10% styrene or divinylbenzene with respect to the surfactant weight. The characteristics of the SANS spectra and the measured bilayer thicknesses are consistent with previously published scattering studies of equilibrium vesicles.[19] Cryo TEM images of vesicles with and without added monomer are also nearly identical. The small dark spots in Figure 3 are ice crystals from frozen condensate inside of the transport dewar that have settled onto the sample grid. These objects are not in focus, and therefore are not in the plane of the vitrified vesicular solution.

Addition of a counterion salt or Triton X-100 to the polymerized vesicle/catanionic surfactant mixtures did not produce clear micellar solutions, as is the case if the vesicles are unpolymerized. Adding salt produces a clear solution over a white precipitate. This is the result of salt micellizing any surfactant unassociated with the polymer shells and subsequent precipitation of the polymer. Precipitation is expected since salt screens the ionic surfactants that act to stabilize the hydrophobic polymer shells. The decrease in scattered intensity upon addition of Triton X-100 also reflects the micellization of the surfactant contained in unpolymerized vesicles. However, Triton X-100 apparently stabilizes the particles and no precipitate forms.

QELS of diluted solutions of sulfonated vesicles (Figure 4) suggests that the equilibrium vesicle form has been captured by polymerization. The polymerized vesicles are robust, and their hydrodynamic radius is independent of dilution, which is different from the behavior of equilibrium vesicles. Unfortunately, QELS does not yield any clues about whether the particles are hollow.

Instead of relying on an electrostatic stabilization of the particles, a nonionic surfactant can be adsorbed to the particle surface to provide a steric stabilization. *N*-Alkyl polyglycol ether surfactants are ideal for this since their amphiphilicity can be systematically adjusted, they are well characterized,[46,47] and contain a hydrophilic group identical to PEG, a moiety shown to protect drug carriers from RES detection in the body.[48−50] *N*-Alkyl polyglycol ether surfactants are denoted as C_iE_j, where "*i*" refers to the number of carbon atoms in the hydrophobic tail and "*j*" refers to the number of ethoxylate units in the hydrophilic head.

The dry polymer shells are redispersed in aqueous solutions of $C_{12}E_8$, $C_{12}E_6$, and $C_{12}E_5$ by simply shaking the mixtures until a clear blue dispersion forms. Polydisperse longer chain amphiphiles such as the Brij surfactants, approximately $C_{18}E_{100}$, $C_{12}E_{23}$, and $C_{18}E_{20}$, require sonication to produce stable dispersions of the polymer shells in water. A minimum ratio of surfactant to polymer particles is required to obtain a one phase solution, or some of the polymer will remain as an unsuspended precipitate (ca. 4 mmol of surfactant/g of polymer).

SANS measurements suggest that polymerization does capture the structure of the equilibrium vesicles. The presence of the q^{-2} region is evidence that the polymer particles are indeed hollow. The fitted model parameters are consistent with previously measured values for the micelle radius[51] and polymerized vesicle radius (from QELS).

Finally, Cryo TEM was used to characterize the $C_{12}E_8$-coated polymer vesicles. The solution used for Cryo TEM is dilute, so only a few polymerized vesicles are visible in each frame, but the hollow shape of the particles is clear

(46) Kahlweit, M.; Strey, R. *Angew. Chem., Int. Ed. Engl.* **1985**, *24*, 654−668.
(47) Schubert, K.-V.; Kaler, E. W. *Ber. Bunsen-Ges. Phys. Chem.* **1996**, *100*, 190−205.
(48) Klibanov, A.; Maruyama, K.; Torchilin, V. P.; Huang, L. *FEBS* **1990**, *268*, 235−237.
(49) Illum, L.; Davis, S. S.; Müller, R. H.; Mak, E.; West, P. *Life Sci.* **1987**, *40*, 367−374.
(50) Illum, L.; Davis, S. S. *FEBS*, **1984** *167*, 79−82.
(51) Corti, N.; Degiorgio, V.; Hayter, J. B.; Zulauf, M. *Chem. Phys. Lett.* **1984**, *109*, 579−583.

(Figure 5). The size (ca. 60 nm radius) of the particles is in good agreement with other measurements. The particles are polydisperse, as are the parent equilibrium vesicles.[17]

It is not possible that the cryo TEM images and SANS spectra of the polymerized structures are simply caused by residual surfactant. If this were the case an increase in the hydrodynamic diameter with dilution would have been observed for the polymerized structures in Figure 4. Additionally, the untreated dry polymeric powder could not be dispersed stably in water even after intense sonication (results not shown). These sonicated mixtures were initially hazy suspensions which always phase separated into a clear aqueous phase above the precipitated polymer. This aqueous phase held no dispersed aggregates (detectable by QELS). Finally, the added C_iE_j surfactant would have micellized surfactant-only vesicles, and the harsh chemistry of sulfonation would have altered the ionic surfactant molecules. Taken together, all of this evidence indicates that the structures observed are the products of polymerization, and cryo TEM shows them to be hollow spheres.

No solid latex particles were observed attached to or within the membranes of the hollow particles, in contrast to the report of Jung et al.[34] However, a population of smaller particles was observed in addition to the hollow particles with Cryo TEM, but no clear image of these structures was obtained. It is possible that these objects include solid latex particles or fragments of polymerized spheres. Fragments of polymer particles could be produced during one of the steps needed to resuspend the hollow spheres. Solid latex particles could also have formed in several ways. Jung et al. suggest that polystyrene latex particles form in their dioctadecyldimethylammonium bromide (DODAB) bilayers because a polymer/surfactant phase separation occurs during polymerization. This results in the formation of "parachutes", an unpolymerized surfactant vesicle attached to a smaller solid polymer latex sphere. The results of our study do not support widespread "parachute" formation during polymerization, since such structures would be destroyed by the dialysis technique, leaving only polymer latex particles to be observed. It is possible such phase separation occurs in a fraction of the vesicles, yielding a polymer latex and polymer shell mixture after dialysis. An alternative explanation for the smaller particles observed is the formation of latex spheres as a result of monomer and initiator reacting in the aqueous domain. This is less plausible given the low solubility of styrene and divinylbenzene in water. In either case, the SANS spectra rule out the possibility that these smaller particles make up a substantial portion of the aggregates in samples containing resuspended hollow particles.

Conclusions

Polydisperse hollow polymer particles have been created from common monomers using catanionic equilibrium vesicle phases as a template for the final microstructure. The particles are robust enough to withstand vacuum-drying and resuspension.

In contrast to the catanionic vesicles formed by the surfactants, the size of the polymerized vesicles is not affected by dilution. This result clearly demonstrates the transformation of an initially fragile aggregation structure into a robust polymer network. Two surface modification strategies were used to stabilize the polymer particles after drying and resuspension in water. One modification relies on sulfonating the aromatic rings of the polymer to create a repulsive electrostatic interaction, and the other modification strategy involves the adsorption of a surfactant that imparts a steric repulsion between the particles. Both methods generate clear blue aqueous solutions of resuspended hollow polymer spheres.

The microstructure of the hollow particles was studied with QELS, SANS, and Cryo TEM. The results are all consistent with a polydisperse suspension of hollow polymer spheres having the same average radius as the initial equilibrium vesicle templates (ca. 60 nm). The bilayer thickness observed with Cryo TEM and SANS varied between 3 and 9 nm and depends on the bilayer composition (e.g., the type of C_iE_j adsorbed). The hollow nature of the particles was most clearly revealed by Cryo TEM and is corroborated by SANS.

Acknowledgment. The authors gratefully recognize funding by NASA Grant NAG3-1955 and NSF Grant CTS-9814399. We acknowledge the support of the National Institute of Standards and Technology, U.S. Department of Commerce, in providing facilities used in this work.

LA000569D